

ORIGINAL ARTICLE

Growth, CO₂ consumption and H₂ production of *Anabaena variabilis* ATCC 29413-U under different irradiances and CO₂ concentrations

H. Berberoğlu¹, N. Barra¹, L. Pilon¹ and J. Jay²

¹ Mechanical and Aerospace Engineering Department, Henry Samueli School of Engineering and Applied Science, University of California Los Angeles, Los Angeles, CA, USA

² Civil and Environmental Engineering Department, Henry Samueli School of Engineering and Applied Science, University of California Los Angeles, Los Angeles, CA, USA

Keywords

carbon dioxide mitigation, cyanobacteria, photobiological hydrogen.

Correspondence

Laurent Pilon, Mechanical and Aerospace Engineering Department, Henry Samueli School of Engineering and Applied Science, University of California Los Angeles, Los Angeles, CA 90095, USA.
E-mail: pilon@seas.ucla.edu

2007/0021: received 9 January 2007, revised 31 May 2007 and accepted 1 July 2007

doi:10.1111/j.1365-2672.2007.03559.x

Abstract

Aims: The objective of this study is to develop kinetic models based on batch experiments describing the growth, CO₂ consumption, and H₂ production of *Anabaena variabilis* ATCC 29413-UTM as functions of irradiance and CO₂ concentration.

Methods and Results: A parametric experimental study is performed for irradiances from 1120 to 16100 lux and for initial CO₂ mole fractions from 0.03 to 0.20 in argon at pH 7.0 ± 0.4 with nitrate in the medium. Kinetic models are successfully developed based on the Monod model and on a novel scaling analysis employing the CO₂ consumption half-time as the time scale.

Conclusions: Monod models predict the growth, CO₂ consumption and O₂ production within 30%. Moreover, the CO₂ consumption half-time is an appropriate time scale for analysing all experimental data. In addition, the optimum initial CO₂ mole fraction is 0.05 for maximum growth and CO₂ consumption rates. Finally, the saturation irradiance is determined to be 5170 lux for CO₂ consumption and growth whereas, the maximum H₂ production rate occurs around 10 000 lux.

Significance and Impact of the Study: The study presents kinetic models predicting the growth, CO₂ consumption and H₂ production of *A. variabilis*. The experimental and scaling analysis methods can be generalized to other microorganisms.

Introduction

Increased amounts of greenhouse gas emissions as well as the exhaustion of easily accessible fossil fuel resources are calling for effective CO₂ mitigation technologies and clean and renewable energy sources. Hydrogen, for use in fuel cells, is considered to be an attractive alternative fuel since water vapour is the only byproduct from its reaction with oxygen. Hydrogen production by cultivation of cyanobacteria in photobioreactors offers a clean and renewable alternative to thermochemical or electrolytic hydrogen production technologies with the added advantage of CO₂ mitigation. In particular, *Anabaena variabilis*

is a cyanobacterium capable of mitigating CO₂ and producing H₂. The objective of this study is to investigate experimentally the CO₂ mitigation, growth, and H₂ production of *A. variabilis* ATCC 29413-UTM in BG-11 medium under atmosphere containing argon and CO₂. Parameters investigated are the irradiance and the initial CO₂ mole fraction in the gas phase.

The cyanobacterium *A. variabilis* is a photosynthetic prokaryote listed among the potential candidates for hydrogen production (Pinto *et al.* 2002), whose genome sequence has been completed (Joint Genome Institute 2007). Moreover, *A. variabilis* and its mutants are of great interest in research as hydrogen producers (Hansel and

Lindblad 1998; Tsygankov *et al.* 1998; Borodin *et al.* 2000; Happe *et al.* 2000; Pinto *et al.* 2002; Yoon *et al.* 2002). *Anabaena variabilis* utilizes light energy in the spectral range from 400 to 700 nm, known as photosynthetically active radiation (PAR), and consumes CO₂ to produce biomass, oxygen and hydrogen. The reader is referred to Refs. (Benemann 2000; Madamwar *et al.* 2000; Das and Veziroglu 2001; Pinto *et al.* 2002; Prince and Kheshgi 2005) for detailed reviews of photobiological hydrogen production. In brief, *A. variabilis* utilizes water as its electron donor (Prince and Kheshgi 2005) and produces hydrogen mainly using nitrogenase enzyme (Madamwar *et al.*, 2000). The primary role of nitrogenase is to reduce nitrogen to ammonia during nitrogen fixation (Das and Veziroglu 2001). H₂ is produced as a by product of this reaction (Das and Veziroglu 2001). In the absence of molecular nitrogen, nitrogenase will reduce protons and catalyze the production of H₂ provided reductants and ATP are present (Das and Veziroglu 2001). Nitrogenase enzyme is located in special cells called heterocysts, which protect nitrogenase from O₂ inhibition (Tsygankov *et al.* 1998). However, at dissolved O₂ concentrations higher than 50 µmol l⁻¹, the produced H₂ is consumed by *A. variabilis* in a reaction catalyzed by the enzyme 'uptake' hydrogenase (Tsygankov *et al.* 1998), thus reducing the net H₂ production rate (Tsygankov *et al.* 1998). Finally, *A. variabilis* also possesses bi-directional hydrogenases located at the cytoplasmic membrane (Madamwar *et al.* 2000). However, unlike nitrogenase, these enzymes are not well protected from oxygen and their functioning is inhibited at relatively low O₂ concentrations (Benemann 2000).

Table 1 summarizes previous studies on H₂ production by *A. variabilis*. It indicates the strain used, the gas phase composition, irradiance and the medium used during growth and H₂ production stages, as well as the specific growth, CO₂ consumption, and H₂ production rates. Briefly, Tsygankov *et al.* (1998) and Sveshnikov *et al.* (1997) studied the hydrogen production by *A. variabilis* ATCC 29413 and by its mutant PK84, lacking the hydrogen uptake metabolism. On the other hand, Markov *et al.* (1993) proposed a two stage photobioreactor alternating between (i) growth and (ii) H₂ production phases for attaining high H₂ production rates. During the growth phase cyanobacteria fix CO₂ and nitrogen from the atmosphere to grow and produce photosynthates. In the H₂ production phase, they utilize the photosynthates to produce H₂. In addition, Yoon *et al.* (2002) used a two stage batch process and suggested an improvement on the first stage by incorporating nitrate in the growth medium for faster growth of *A. variabilis*. As opposed to using a two stage photobioreactor, Markov *et al.* (1997b) demonstrated a single stage photobioreactor using *A. variabilis*

PK-84 in a helical photobioreactor. More recently, Tsygankov *et al.* (2002) demonstrated a single stage photobioreactor operation for H₂ production using *A. variabilis* PK-84 in an outdoor photobioreactor similar to that of Markov *et al.* (1997b).

Most previous studies using *A. variabilis* have used a two stage photobioreactor with relatively limited ranges of CO₂ concentrations and light irradiance. In addition, to the best of our knowledge, there has been no reported study simultaneously varying irradiance and the initial CO₂ mole fraction in the gas phase to assess quantitatively the CO₂ mitigation, growth, and H₂ production of *A. variabilis* in a single stage process. The objectives of this work are (i) to develop kinetic models based on batch experiments describing the growth, CO₂ consumption and H₂ production of *A. variabilis* ATCC 29413-UTM as functions of irradiance and CO₂ concentration and (ii) to provide recommendations on the optimum irradiance and the gas phase CO₂ mole fraction for achieving rapid growth, high CO₂ uptake and H₂ production rates.

Materials and methods

A cyanobacterial suspension was prepared from a 7-day-old culture. The micro-organism concentration denoted by X was adjusted to 0.02 kg dry cell m⁻³ by diluting the culture with fresh medium and was confirmed by monitoring the optical density (OD). Then, 60 ml of the prepared suspension was dispensed in 160-ml serum vials. The vials were sealed with butyl rubber septa, crimped and flushed through the septa with industrial grade argon, sterilized with 0.2 µm pore size syringe filter, for 10 min with a needle submerged in the liquid phase. The initial CO₂ mole fraction in the head-space, denoted by $x_{\text{CO}_2, \text{gas}}$, was set at 0.03, 0.04, 0.08, 0.15 and 0.20. This was achieved first by adjusting the gauge pressure in the vials to -7.09, -10.13, -20.27, -30.40 and -40.53 kPa respectively. Then, 7, 10, 20, 30 and 40 ml of industrial grade CO₂ were injected into the vials, respectively, through a 0.2 µm pore size syringe filter. The vials were shaken until the head-space pressure stabilized indicating that both the partitioning of CO₂ between the gas and liquid phases and the dissolution of CO₂ in water were at equilibrium. Finally, the head-space was sampled to measure the initial CO₂ mole fraction. Each vial was prepared in duplicates. The vials were placed horizontally on an orbital shaker (model ZD-9556 by Madell Technology Group, Orange County, CA, USA) and stirred continuously at 115 rev min⁻¹ throughout the duration of the experiments. Continuous illumination was provided from the top of the orbital shaker. The transparent glass vials could be approximated to a cylindrical tube of diameter 50 mm, of height 80 mm, and of wall thickness 2 mm. The illuminated surface area of each

Table 1 Summary of experimental conditions used and associated maximum specific growth, CO₂ consumption and H₂ production rates reported in the literature using various strains of *Anabaena variabilis*

<i>A. variabilis</i> strain	Stage I			Stage II			Maximum reported rates			
	Gas phase	Medium	Irradiance (lux)	Gas phase	Medium	Irradiance (lux)	μ (h ⁻¹)	ψ_{CO_2} (mmol/kg dry cell/h)	π_{H_2} (mmol/kg dry cell/h)	References
Kutzung 1403/4B	95 vol.% air + 5 vol.% CO ₂	Allen and Arnon w/o nitrate at 25°C	1800	300 mm Hg vacuum	Same as stage I	13 000	N/A	7000	830	(Markov et al. 1995)
ATCC 29413	89 vol.% air + 11 vol.% CO ₂	BG-11 _o + 3.5 mmol l ⁻¹ NaNO ₃ at 30°C	2500–5500	Argon	BG-11 _o w/o nitrate at 30°C	9000–12 000	0.05	2700	80	(Yoon et al. 2002)
ATCC 29413	98 vol.% air + 2 vol.% CO ₂	Allen and Arnon w/o nitrate molybdenum replaced w/vanadium at 30°C	8000	Argon	Same as stage I	10 000–14 000	N/A	N/A	630	(Tsygankov et al. 1998)
PK 84	98 vol.% air + 2 vol.% CO ₂	Allen and Arnon w/o nitrate molybdenum replaced w/vanadium at 30°C	8000	Argon	Same as stage I	10 000–14 000	N/A	N/A	515	(Tsygankov et al. 1998)
ATCC 29413	73 vol.% Ar + 25 vol.% N ₂ + 2 vol.% CO ₂	Allen and Arnon w/o nitrate molybdenum replaced w/vanadium at 30°C	6500	93 vol.% Ar + 5 vol.% N ₂ + 2 vol.% CO ₂	Same as stage I	6500	N/A	N/A	720/37	(Sveshnikov et al. 1997)
PK 84	73 vol.% Ar + 25 vol.% N ₂ + 2 vol.% CO ₂	Allen and Arnon w/o nitrate molybdenum replaced w/vanadium at 30°C	6500	93 vol.% Ar + 5 vol.% N ₂ + 2 vol.% CO ₂	Same as stage I	6500	N/A	N/A	2600	(Sveshnikov et al. 1997)
PK 84	98 vol.% air + 2 vol.% CO ₂	Allen and Arnon w/o nitrate molybdenum replaced w/vanadium at 30°C	outdoor	98 vol.% Air + 2 vol.% CO ₂	Same as stage I	Outdoor	0.03	N/A	300	(Tsygankov et al. 2002)

vial was $40 \times 10^{-4} \text{ m}^2$. The irradiance, defined as the total radiant flux of visible light from 400 to 700 nm incident on a vial from the hemisphere above it, ranged from 1120 to 16 100 lux. Note that for the lamps used in the experiments 1 lux of irradiance was equivalent to $3 \times 10^{-3} \text{ W m}^{-2}$ and $14 \times 10^{-3} \mu\text{mol m}^{-2} \text{ s}^{-1}$ in the PAR.

Throughout the experiments CO₂, H₂ and O₂ concentrations in the head-space as well as the cyanobacteria concentration and pH in the liquid phase were continually monitored. In addition, the temperature and pressure of the vials were measured to convert the molar fractions of gas species into volumetric mass concentrations. The irradiance incident on individual vials was recorded. Details of the experimental setup and procedures are given in the following sections.

Cyanobacteria culture and concentration measurements

Anabaena variabilis ATCC 29413-UTM was purchased from the American Type Culture Collection (ATCC) and received in freeze dried form. The culture was activated with 10 ml of sterilized milli-Q water. It was cultivated and transferred weekly in ATCC medium 616 with air-CO₂ mixture in the head-space with an initial mole fraction of CO₂ of 0.05. One litre of ATCC medium 616 contained 1.5 g NaNO₃, 0.04 g K₂HPO₄, 0.075 g MgSO₄·7H₂O, 0.036 g CaCl₂·2H₂O, 6.0 mg citric acid, 6.0 mg ferric ammonium citrate, 0.02 g Na₂CO₃, 1.0 mg EDTA and 1.0 ml of trace metal mix A5. One litre of trace metal mix A5 contains 2.86 g H₃BO₃, 1.81 g MnCl₂·4H₂O, 0.222 g ZnSO₄·7H₂O, 0.39 g Na₂MoO₄·2H₂O, 0.079 g CuSO₄·5H₂O, 49.4 mg Co(NO₃)₃·6H₂O. The pH of the medium was adjusted to be 7.3 by adding 1 mol l⁻¹ HCl and/or 1 mol l⁻¹ NaOH. Then, 20 ml of HEPES buffer solution at pH 7.3 was added to one litre of medium. Finally, the medium was autoclaved at 121°C for 40 min.

The cyanobacteria concentration *X* was determined by sampling 1 ml of bacteria suspension from the vials and measuring the OD. A calibration curve was created by measuring both the dry cell weight of a cyanobacteria suspension and the corresponding OD. First, the OD of the cyanobacteria was measured in disposable polystyrene cuvettes with light path of 10 mm at 683 nm (Yoon *et al.* 2002) using a UV-Vis spectrophotometer (Cary-3E; Varian, Palo Alto, CA, USA). Then, the bacteria suspension was filtered through mixed cellulose filter membranes with 0.45 μm pore size (HAWP-04700; Millipore, Billerica, MA, USA) and dried at 85°C over night. The dried filters were weighed immediately after being taken out of the oven on a precision balance (model AT261; Delta Range Factory, USA) with a precision of 0.01 mg. The calibration curve for OD was generated by using 14

different bacteria concentrations ranging from 0.04 to 0.32 kg dry cell m⁻³. The relation between OD and bacteria concentration is linear for the OD range from 0 to 1.2 and 1 unit of OD corresponds to 0.274 kg dry cell m³.

Temperature, pressure and pH

The temperature of the vials was measured with a thermocouple (Dual Thermometer; Fisher Scientific, Houston, TX, USA). The heat from the high intensity fluorescent bulbs was removed by convective cooling using a fan to maintain a steady-state temperature of $24 \pm 1^\circ\text{C}$ throughout the duration of the experiments. The head-space pressure was monitored with a digital gauge pressure sensor (model PX26-005GV; Omega Engineering Inc., Stanford, CT) connected to a digital meter (model DP25B-S by Omega Heater Company). Finally, the pH of the medium was measured with a digital pH probe (model Basic AB Plus; Fisher Scientific).

Lighting and light analysis

The irradiance incident on the vials G_{in} was provided by fluorescent light bulbs (Ecologic by Sylvania, USA and Fluorex by Lights of America, USA) and varied by changing the number of bulbs. The spectral irradiance of these bulbs was measured with a spectrophotometer (model USB2000, Ocean Optics, Dunedin, FL) connected to a cosine collector over the spectral range from 350 to 750 nm. The spectral irradiance of the light bulbs G_{λ} , normalized with its maximum value G_{max} at 540 nm, along with the reported cyanobacterial absorption coefficient κ_{λ} (Merzlyak and Naqvi 2000), normalized with its maximum value κ_{max} , are presented in Fig. 1. The irradiance incident on the vials was measured with both a light meter (Fisherbrand Tracable Meter by Fisher Scientific) and a quantum sensor (LI-COR, Model LI-190SL; LI-COR Inc., Lincoln, NE, USA). The total irradiance on each vial was measured individually in the PAR, i.e. within the spectral range from 400 to 700 nm. Due to experimental difficulties in achieving the exact same irradiance for all vials, five different irradiance ranges were explored namely, 1120–1265, 1680–2430, 3950–4600, 7000–8700 and 14 700–16 100 lux.

Gas analysis

The gas analysis was carried out every 24 h by sampling 500 μl of head-space volume of the vials. The concentrations of CO₂, H₂ and O₂ in the head-space were measured with a gas chromatographer (HP-5890; Hewlett Packard, Palo Alto, CA) equipped with a packed column (Carboxen-1000; Supelco, Bellefonte, PA, USA) and a

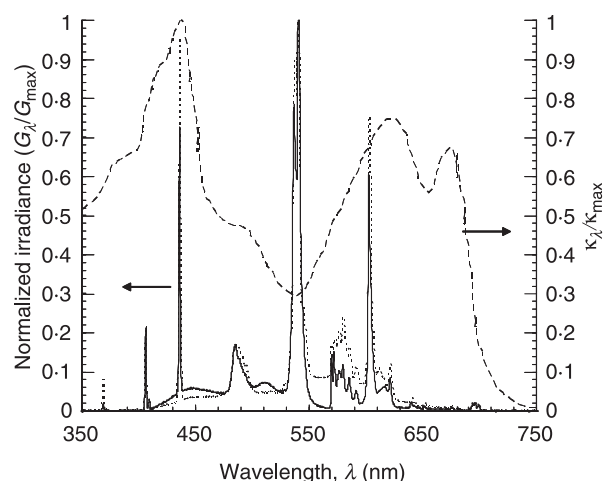


Figure 1 The normalized spectral irradiance of Ecologic (solid line) and Fluorex (dotted line) light bulbs G_{λ}/G_{\max} along with the normalized absorption coefficient of *Anabaena variabilis* (dashed line) $\kappa_{\lambda}/\kappa_{\max}$ (Merzlyak and Naqvi 2000).

thermal conductivity detector (TCD). The gas chromatographer output was processed with an integrator (HP-3395, Hewlett Packard). Throughout the gas analysis, the injector and detector temperatures were maintained at 120°C. During the H₂ and O₂ analysis argon was used as the carrier gas and the oven temperature was maintained at 35°C. The retention times for H₂ and O₂ were found to be 2.1 and 7.5 min respectively. On the other hand, during the CO₂ analysis, Helium was used as the carrier gas and the oven temperature was maintained at 255°C. The retention time for CO₂ was then 4.9 min. Calibration curves for the TCD response were prepared at seven

different known gas concentrations from 16×10^{-6} to 3.2×10^{-3} kg m⁻³ for H₂, from 25.6×10^{-3} to 1314×10^{-3} kg m⁻³ for O₂ and from 3.96×10^{-3} to 352×10^{-3} kg m⁻³ for CO₂. All calibration curves were linear within these gas concentration ranges. During the experiments, peak heights were recorded and correlated with the corresponding moles of gas using the respective calibration curves.

Results

The experimental parameters used in the study along with the experimental labels are summarized in Table 2. In brief, the initial CO₂ mole fraction in the head-space, $x_{\text{CO}_2, \text{g}, 0}$, varied from 0.03 to 0.20 while the irradiance G varies from 1120 to 16 100 lux. Pressure, temperature and pH were maintained at 1 ± 0.1 atm., $24 \pm 1^\circ\text{C}$ and 7.0 ± 0.4 , respectively. To develop semi-empirical models for CO₂ consumption, growth, H₂ and O₂ production by *A. variabilis* ATCC 29413 using the experimental data, the following assumptions are made:

1. The concentration of gases in each phase and the concentration of cyanobacteria in the liquid phase are uniform within a given vial, due to vigorous mixing provided by the orbital shaker.
2. The Damkohler number, defined as the ratio of the reaction rate to the mass transfer rate (Smith *et al.* 1998), associated with the experimental setup is on the order of 10^{-4} . Therefore, metabolic reactions of the cyanobacteria are not mass transfer limited (Smith *et al.* 1998).
3. The gas species in the liquid and gas phases are at quasi-equilibrium at all times.

Table 2 Summary of the parameters used in the experiments

Label	G (lux)	$x_{\text{CO}_2, \text{g}, 0}$	$t_{1/2}$ (h)	μ_{avg} (h ⁻¹)	Y_{X/CO_2} (kg kg ⁻¹)	ψ_{CO_2} (kg kg ⁻¹ h ⁻¹)
0GH	7000	0.20	74.4	0.024	0.373	0.065
0IJ	14 700	0.20	65.3	0.028	0.352	0.081
1AB	1120	0.15	232.8	0.009	0.451	0.020
1CD	1680	0.15	189.3	0.013	0.589	0.023
1EF	3950	0.15	82.3	0.024	0.465	0.051
1GH	8700	0.15	49.5	0.033	0.398	0.082
1IJ	16 100	0.15	46.8	0.036	0.381	0.094
2AB	1175	0.08	120.6	0.013	0.555	0.024
2CD	1820	0.08	98.4	0.016	0.626	0.026
2EF	4300	0.08	53.2	0.027	0.489	0.055
2GH	8000	0.08	37.1	0.038	0.440	0.086
2IJ	16 100	0.08	39.1	0.041	0.433	0.094
3AB	1195	0.04	71.4	0.018	0.685	0.026
3CD	1815	0.04	57.3	0.022	0.755	0.030
3EF	4190	0.04	32.0	0.037	0.629	0.059
4AB	1265	0.03	64.9	0.017	0.840	0.020
4CD	2430	0.03	73.8	0.023	0.859	0.026
4EF	4600	0.03	27.3	0.029	0.748	0.038

4. *A. variabilis* both consumes and produces CO₂, O₂ and H₂. Therefore, the reported gas phase concentration of species correspond to the net consumed or produced quantities.

5. The only parameters affecting the bacterial growth and product formation are the CO₂ concentration and the irradiance *G*. The supply of other nutrients such as minerals and nitrate are assumed to be unlimited in the growth medium.

6. Given the pH range, the effect of buffer capacity on the growth rate is assumed to be negligible compared with the effects of CO₂ concentration and local irradiance.

7. The death of micro-organisms is neglected within the time frame of the experiments.

Kinetic modelling

During the growth phase, the time rate of change of micro-organism concentration *X* can be written as (Dunn *et al.* 2003),

$$\frac{dX}{dt} = \mu X, \quad (1)$$

where μ is the specific growth rate of the cyanobacteria expressed in s⁻¹. In this study, it is assumed to be a function of (i) the average available irradiance denoted by G_{av} and (ii) the concentration of total dissolved inorganic carbon within the cyanobacterial suspension denoted by C_{TOT} . The specific growth rate has been modelled using the Monod model taking into account (i) light saturation; (ii) CO₂ saturation; and (iii) CO₂ inhibition as (Asenjo and Merchuk 1995):

$$\mu = \mu_{max} \left(\frac{G_{av}}{G_{av} + K_G} \right) \left(\frac{C_{TOT}}{K_C + C_{TOT} + C_{TOT}^2/K_I} \right), \quad (2)$$

where μ_{max} is the maximum specific growth rate, K_G is the half-saturation constant for light, K_C and K_I are the half-saturation and the inhibition constants for dissolved inorganic carbon respectively. First, the spectral and local irradiance $G_\lambda(z)$ within the suspension is estimated using Beer–Lambert's law as:

$$G_\lambda(z) = G_{\lambda,in} \exp(-E_{ext,\lambda} X z), \quad (3)$$

where $G_{\lambda,in}$ is the spectral irradiance incident on the vials, z is the distance from the top surface of the suspension, X is the micro-organism concentration in kg dry cell m⁻³, $E_{ext,\lambda}$ is the spectral extinction cross-section of *A. variabilis* at wavelength λ . Note that $E_{ext,\lambda}$ varies by <4% over the PAR and is assumed to be constant and equal to $E_{ext,PAR} = 350 \text{ m}^2 \text{ kg}^{-1}$ dry cell (Berberoğlu and Pilon 2007). Then, the available irradiance G_{av} can be estimated by averaging the local irradiance over the depth of the culture L as:

$$G_{av} = \frac{1}{L} \int_0^L G(z) dz \quad \text{where} \quad G(z) = G_{in} \exp(-E_{ext,PAR} X z), \quad (4)$$

Experimentally L is equal to 0.02 m.

Finally, C_{TOT} is the total dissolved inorganic carbon concentration in the liquid phase expressed in kmol m⁻³. It depends on the pH of the medium and on the molar fraction of CO₂ in the gas phase $x_{CO_2,g}$ and can be written as (Benjamin 2002):

$$C_{TOT} = 10^{-1.5} x_{CO_2,g} + \left(\frac{10^{-7.8}}{10^{-pH}} \right) x_{CO_2,g} + \left(\frac{10^{-28.1}}{10^{-2pH}} \right) x_{CO_2,g}, \quad (5)$$

where the three terms on the right hand side correspond to H₂CO₃^{*}, HCO₃⁻, and CO₃²⁻ concentrations in the liquid phase respectively.

The values of the parameters μ_{max} , K_G , K_C , and K_I in eqn (2) are estimated by minimizing the root mean square error between the experimentally measured cyanobacteria concentrations and the model predictions obtained by integrating eqns (1) and (2). The associated parameters along with those reported by Erickson *et al.* (1987) for the cyanobacteria *Spirulina platensis* are summarized in Table 3. Figure 2a compares the cyanobacteria concentrations measured experimentally with the model predictions. It indicates that the model predicts the experimental data for micro-organism concentration within 30%.

Moreover, assuming that the biomass yield based on consumed carbon and denoted by $Y_{X/C}$ is constant, as assumed by Erickson *et al.* (1987), the total dissolved inorganic carbon concentration can be modelled as (Dunn *et al.* 2003):

$$\frac{dC_{TOT}}{dt} = -\frac{\mu}{Y_{X/C}} X, \quad (6)$$

The yield $Y_{X/C}$ can be expressed in terms of the biomass yield based on consumed CO₂ denoted by Y_{X/CO_2} as $Y_{X/C} = M_{CO_2} Y_{X/CO_2}$ where M_{CO_2} is the molecular weight of

Table 3 Summary of the parameters used in kinetic modeling of *Anabaena variabilis*

Parameter	Present study	Erickson <i>et al.</i> (1987)	Equation
μ_{max} (1 h ⁻¹)	0.10	0.12	Eqn (2)
K_G (lux)	4440	4351	Eqn (2)
K_C (kmol C m ⁻³)	0.0002	0.0002	Eqn (2)
K_I (kmol C m ⁻³)	0.0182	N/A	Eqn (2)
$Y_{X/C}$ (kg dry cell kmol ⁻¹ C)	24.96	25.18	Eqn (6)
Y_{O_2X} (kg O ₂ kg ⁻¹ dry cell)	1.28	N/A	Eqn (7)

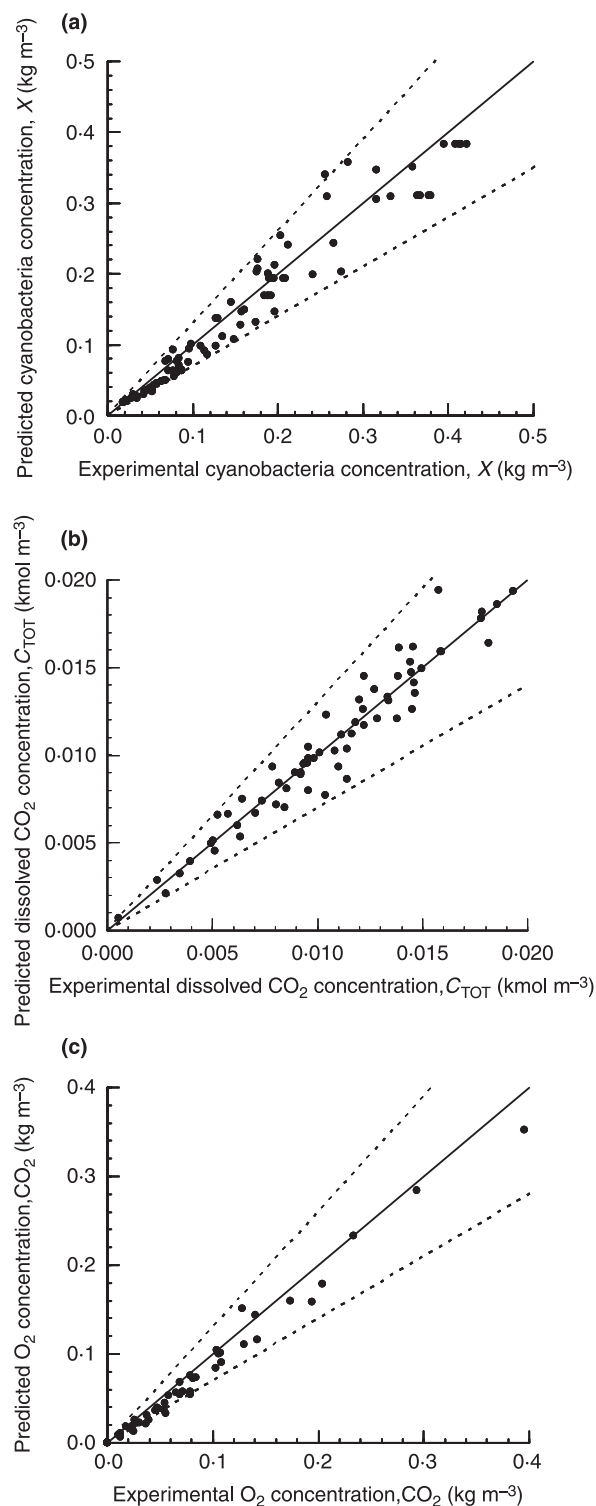


Figure 2 Comparison between experimental data and kinetic model predictions for (a) cyanobacterial concentration (eqn 2), (b) total dissolved inorganic carbon concentration (eqn 6) and (c) total O₂ concentration (eqn 7). The dashed lines correspond to ±30% deviation from model predictions.

CO₂ equal to 44 kg kmol⁻¹. The value of Y_{X/CO_2} for each experiment is given in Table 2. The value of $Y_{X/C}$ used in this study is the average value obtained across experiments which is equal to 24.96 kg dry cell kmol⁻¹ C. Figure 2b compares C_{TOT} obtained using eqn (5) and the measured pH and $x_{CO_2,g}$ with the value predicted by integrating eqn (6). It shows that the model predicts the experimental data within 30%.

Furthermore, assuming that one mole of O₂ is evolved per mole of CO₂ consumed, the total oxygen concentration in the vial can be computed as,

$$\frac{dC_{O_2}}{dt} = Y_{O_2/X} \mu X, \quad (7)$$

where $Y_{O_2/X}$ is the O₂ yield based on biomass and equal to 1.28 kg O₂ kg⁻¹ dry cell. It is expressed as $M_{O_2}/Y_{X/C}$ where M_{O_2} is the molecular weight of O₂ equal to 32 kg kmol⁻¹. Figure 2c compares the total O₂ concentration measured experimentally with that predicted by integrating eqn (7). It indicates that the experimental data for C_{O₂} falls within 30% of model's predictions.

Finally, models similar to eqns (6) and (7) were applied to the H₂ concentration in the headspace measured as a function of time. However, yield coefficients could not be obtained to model the experimental data within 30%.

Scaling analysis

The models described in the previous section depend on quantities such as G_{av} and C_{TOT} that are not directly measurable. They are typically kept constant by using either a chemostat (Erickson *et al.* 1987) or a turbidostat (Goldman *et al.* 1974). However, construction and operation of these devices are relatively expensive and experimentally more challenging than the vial experiments performed in this study. Moreover, a number of assumptions had to be made to estimate the parameters of the kinetic models. Specifically, G_{av} was estimated using Beer-Lambert's law which does not take into account in-scattering by the micro-organisms and can lead to errors as high as 30% in estimating the local irradiance $G_L(z)$ (Berberoğlu *et al.* 2007). Moreover, the growth rates of the micro-organisms were assumed to be independent of pH which varied between 7.0 ± 0.4 during the course of the experiments. Furthermore, the average yields $Y_{X/C}$ and $Y_{O_2/X}$ were assumed to be constant in modeling the CO₂ consumption and O₂ production. Finally, modeling H₂ production with the approach above gave poor results. Therefore, as an alternative to the kinetic models described above, a novel scaling analysis is presented for analysing the data based on the directly measurable initial molar fraction $x_{CO_2,g,0}$ and incident irradiance G_{in} while G_{av} and C_{TOT} are allowed to vary with time.

CO₂ consumption

Figure 3a shows the evolution of the CO₂ molar fraction $x_{\text{CO}_2,\text{g}}$ in the head-space as a function of time t , normalized with the initial CO₂ mole fraction $x_{\text{CO}_2,\text{g},0}$ for different combinations of the total incident irradiance G_{in} and $x_{\text{CO}_2,\text{g},0}$. It indicates that $x_{\text{CO}_2,\text{g}}$ decreases monotonically with increasing time. First, the half-time, denoted by $t_{1/2}$, is defined as the time required for the CO₂ mole fraction in the gas phase to decrease to half of its initial value. Normalizing the time by the half-time and plotting the dimensionless variables $x_{\text{CO}_2,\text{g}}/x_{\text{CO}_2,\text{g},0}$ vs $t/t_{1/2}$, collapses all the data points to a single line as shown in Fig. 3b. This

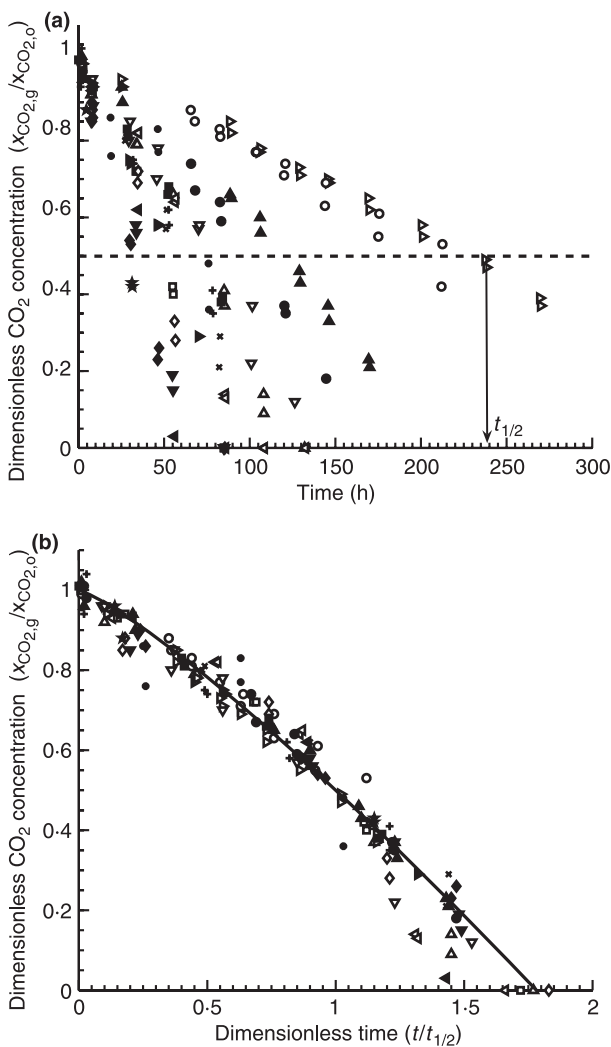


Figure 3 (a) Normalized CO₂ consumption data vs time, (b) normalized CO₂ consumption data vs dimensionless time for (Δ) 0GH, (◁) 0IJ, (▽) 1AB, (○) 1CD, (▽) 1EF, (□) 1GH, (◇) 1IJ, (▲) 2AB, (●) 2CD, (◄) 2EF, (▼) 2GH, (▶) 2IJ, (■) 3AB, (×) 3CD, (◆) 3EF, (+) 4AB, (★) 4CD, (★) 4EF. The solid line corresponds to $x_{\text{CO}_2,\text{g}}/x_{\text{CO}_2,\text{g},0} = 1 - 0.5(t/t_{1/2})^{1.2}$.

indicates that the CO₂ consumption half time is an appropriate time scale for comparing CO₂ consumption under different conditions. Performing a linear regression analysis of the data yields:

$$\frac{x_{\text{CO}_2,\text{g}}}{x_{\text{CO}_2,\text{g},0}} = 1 - 0.5 \left(\frac{t}{t_{1/2}} \right)^{1.2}, \quad (8)$$

with a correlation coefficient $R^2 = 0.94$. Equation (8) also indicates that $x_{\text{CO}_2,\text{g}}$ vanishes at time $t = 1.8t_{1/2}$.

Moreover, the half-time $t_{1/2}$ is a function of both the initial CO₂ mole fraction and the irradiance G_{in} . Figure 4a shows $t_{1/2}$ as a function of $x_{\text{CO}_2,\text{g},0}$ for different values of G_{in} . It indicates that $t_{1/2}$ increases linearly with $x_{\text{CO}_2,\text{g},0}$ for a given G_{in} , i.e. $t_{1/2} = \beta(G_{\text{in}})x_{\text{CO}_2,\text{g},0}$, where the slope $\beta(G_{\text{in}})$ is expressed in hours and plotted in Fig. 4b. Two regimes can be identified. In the first regime, $\beta(G_{\text{in}})$ decreases linearly with G_{in} according to $\beta(G_{\text{in}}) = 1900 - 0.3G_{\text{in}}$. In the second regime, $\beta(G_{\text{in}})$ does not vary appreciably with G_{in} and has the approximate value of 350 h. Figure 4b indicates that transition between the two regimes occurs around $G_{\text{in}} = 5170$ lux. Therefore, the half-time $t_{1/2}$ can be expressed as:

$$\begin{aligned} t_{1/2} &= (1900 - 0.3G_{\text{in}})x_{\text{CO}_2,\text{g},0} & \text{for } G_{\text{in}} \leq 5170 \text{ lux} \\ t_{1/2} &= 350x_{\text{CO}_2,\text{g},0} & \text{for } G_{\text{in}} > 5170 \text{ lux} \end{aligned} \quad (9)$$

Alternatively, the relationship between β and G_{in} can be approximated with an exponential decay function as $\beta(G_{\text{in}}) = 350 + 1300\exp(9 \times 10^{-8}G_{\text{in}}^2)$.

Furthermore, Fig. 5a compares the values of experimentally determined $t_{1/2}$ with those predicted by eqn (9). With the exception of one outlier, all the experimentally determined half-times lie within ± 20 h of the predictions by eqn (9). The experimental values of $t_{1/2}$ and t_d are summarized in Table 2 for each test.

In addition, Fig. 5b shows the medium pH as a function of the dimensionless time $t/t_{1/2}$ for all runs. It shows that the medium pH increases as the CO₂ is consumed by the micro-organisms. It also indicates that the pH changes also scale well with the time scale $t_{1/2}$.

Cyanobacterial growth

Figure 6a, b show the normalized concentration of *A. variabilis*, X/X_0 , vs time t for all irradiances and for $x_{\text{CO}_2,\text{g},0} = 0.08$ and 0.15 respectively. The initial cyanobacteria concentration X_0 is equal to 0.02 kg dry cell m⁻³ in all cases. Figure 6 establishes that for a given $x_{\text{CO}_2,\text{g},0}$, increasing the irradiance increases the growth rate of *A. variabilis*. Moreover, for a given irradiance G_{in} within the values tested, decreasing the initial CO₂ mole fraction increases the growth rate. Thus, the effects of G_{in} and $x_{\text{CO}_2,\text{g},0}$ on cyanobacterial growth seem to be coupled.

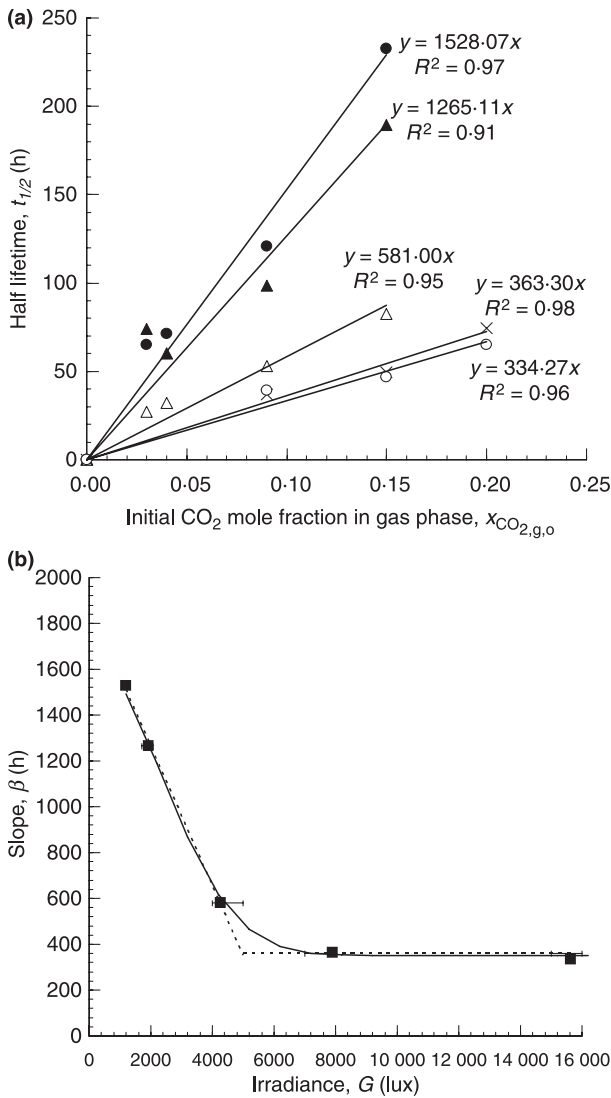


Figure 4 (a) Half-time as a function of $x_{\text{CO}_{2,g,0}}$ for (●) 1100–1200 lux, (▲) 1700–1800 lux, (△) 4000–5000 lux, (×) 7000–8000 lux, and (○) 15 000–16 000 lux. (b) Slope β as a function of irradiance G . The solid line corresponds to $\beta = 350 + 1300\exp(-9 \times 10^{-8}G^2)$.

Here also, scaling the time with the half-time $t_{1/2}$ collapses the growth curves for different irradiances onto a single line as shown in Fig. 6c, d for $x_{\text{CO}_{2,g,0}} = 0.08$ and 0.15 respectively. Therefore, the half-time $t_{1/2}$ correctly captures the time scale of the biological processes for CO₂ consumption and bacterial growth. In addition, the cyanobacterial growth is exponential and the cyanobacteria concentration $X(t)$ at time t can be expressed as:

$$\frac{X(t)}{X_0} = \exp\left(\frac{\alpha}{t_{1/2}}t\right), \quad (10)$$

where α is a constant depending on $x_{\text{CO}_{2,g,0}}$ and determined experimentally. Figure 7 shows its evolution as a

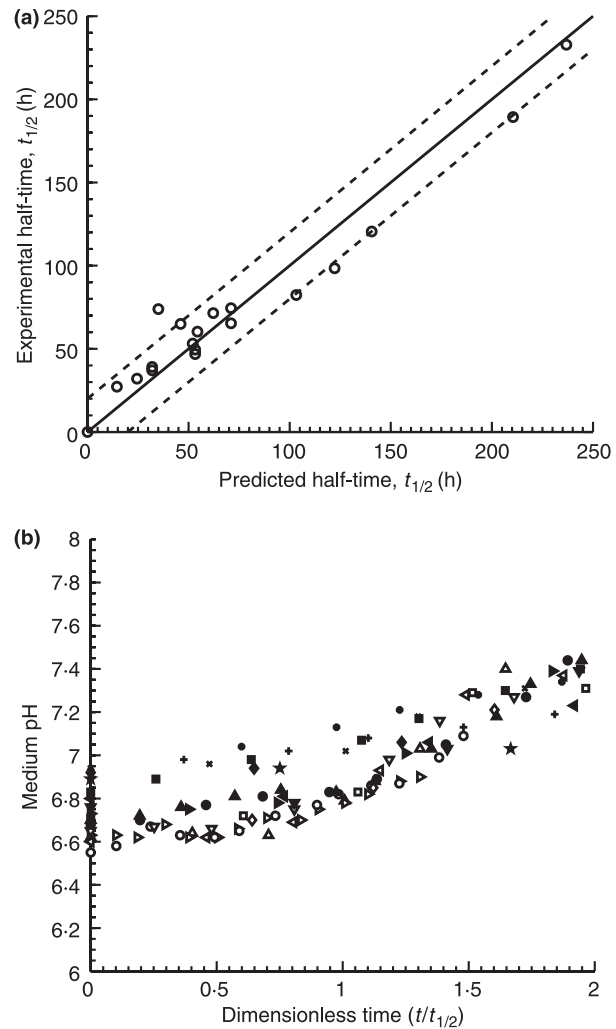


Figure 5 (a) Comparison of experimental vs predicted half-times. The solid line corresponds to the model $t_{1/2} = (1900 - 0.3G)x_{\text{CO}_{2,g,0}}$ and the dashed lines correspond to $\pm 20\%$ -deviations from the model. (b) The medium pH as a function of the dimensionless time $t/t_{1/2}$ for (△) 0GH, (<) 0IJ, (▷) 1AB, (○) 1CD, (▽) 1EF, (□) 1GH, (<◁) 1IJ, (▲) 2AB, (●) 2CD, (◀) 2EF, (▼) 2GH, (▶) 2IJ, (■) 3AB, (×) 3CD, (◆) 3EF, (+) 4AB, (★) 4CD, (☆) 4EF.

function of $x_{\text{CO}_{2,g,0}}$ varying between 0.03 and 0.20. The relationship can be expressed as:

$$\alpha = 4x_{\text{CO}_{2,g,0}}^{0.35} \quad (11)$$

with a correlation coefficient $R^2 = 0.93$. Note that the evolution of $X(t)$ as a function of the irradiance G_{in} and $x_{\text{CO}_{2,g,0}}$ is accounted for through the half-time $t_{1/2}$ given by eqn (9).

Moreover, the average specific growth rate, denoted by μ_{avg} , is the arithmetic mean of the specific growth rates, denoted by $\mu_{\Delta t}$ and determined in the time interval Δt

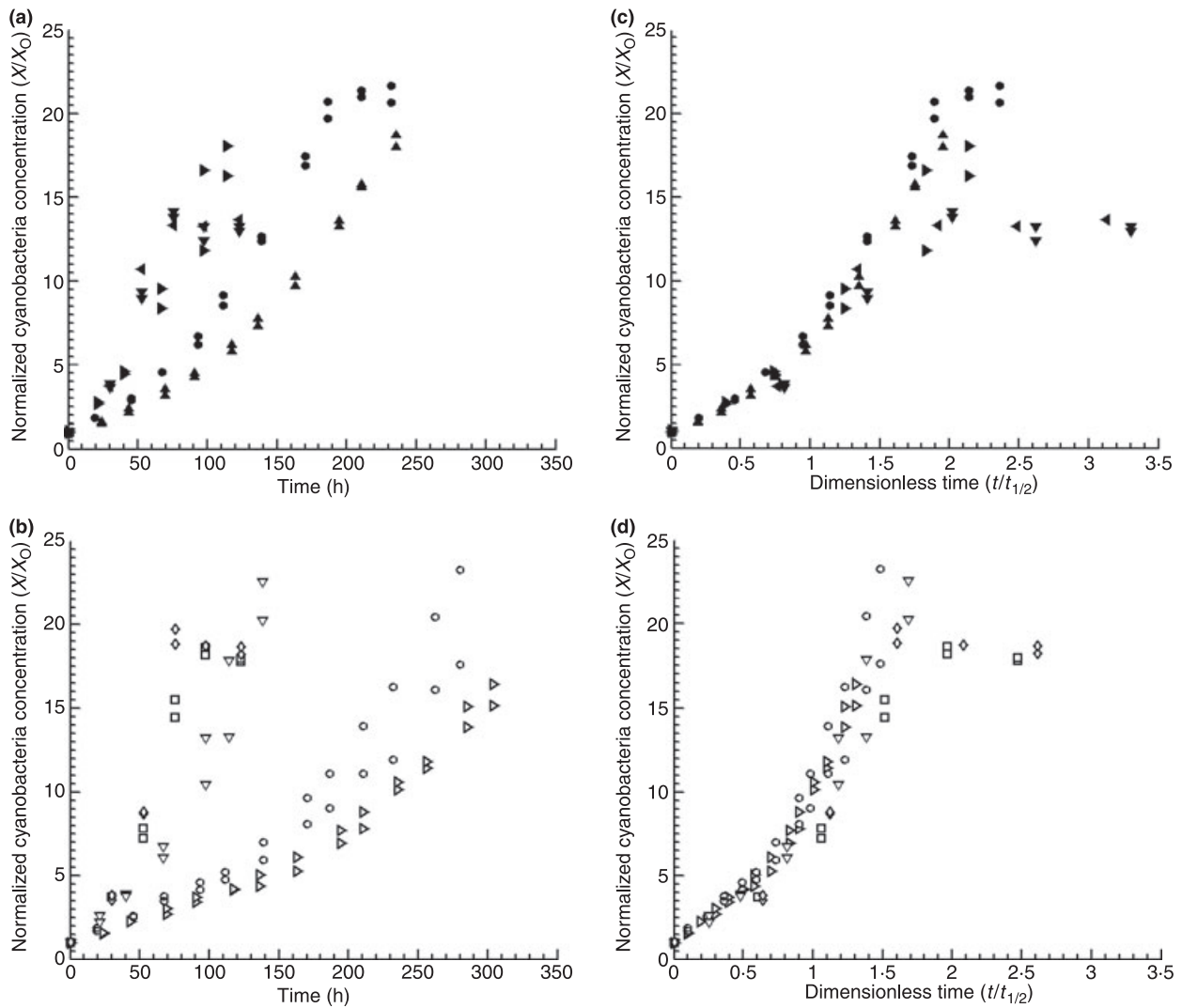


Figure 6 Normalized cyanobacteria concentrations at all irradiances as functions of time for (a) $x_{\text{CO}_{2,g,0}}=0.08$ and (b) $x_{\text{CO}_{2,g,0}}=0.15$. Normalized cyanobacteria concentrations at all irradiances as functions of dimensionless time for (c) $x_{\text{CO}_{2,g,0}}=0.08$ and (d) $x_{\text{CO}_{2,g,0}}=0.15$ for (▲) 2AB, (●) 2CD, (□) 2EF, (▼) 2GH, (◀) 2IJ, (▷) 1AB, (○) 1CD, (▽) 1EF, (◻) 1GH, (◇) 1IJ.

during the exponential growth phase of *A. variabilis* according to (Yoon *et al.* 2002):

$$\mu_{\Delta t} = \frac{\Delta X}{\Delta t} \frac{1}{X_{\text{avg},\Delta t}}, \quad (12)$$

where $X_{\text{avg},\Delta t}$ is the arithmetic mean of the cyanobacteria concentration during that time interval Δt . The values of μ_{avg} computed for all parameters are summarized in Table 2. Figure 8a presents the variation of the average specific growth rate of *A. variabilis* denoted by μ_{avg} and expressed in h^{-1} , as a function of $x_{\text{CO}_{2,g,0}}$ for all irradiances. The error bars indicate the standard error that is the ratio of the standard deviation to the square root of the number of samples.

Furthermore, the average specific CO₂ uptake rate, denoted by ψ_{CO_2} and expressed in $\text{kg kg}^{-1} \text{ dry cell h}^{-1}$, is computed using the same method as that used by Yoon *et al.* (2002):

$$\psi_{\text{CO}_2} = \frac{\mu_{\text{avg}}}{Y_{X/\text{CO}_2}}, \quad (13)$$

where Y_{X/CO_2} is the biomass yield based on consumed CO₂ expressed in $\text{kg dry cell kg}^{-1}$ of CO₂. It is computed as the ratio of the final mass of cyanobacteria produced to the total mass of CO₂ injected into the vials. The values of ψ_{CO_2} computed for all parameters are also summarized in Table 2. Figure 8b shows the variation of ψ_{CO_2} as a function of $x_{\text{CO}_{2,g,0}}$ for all irradiances.

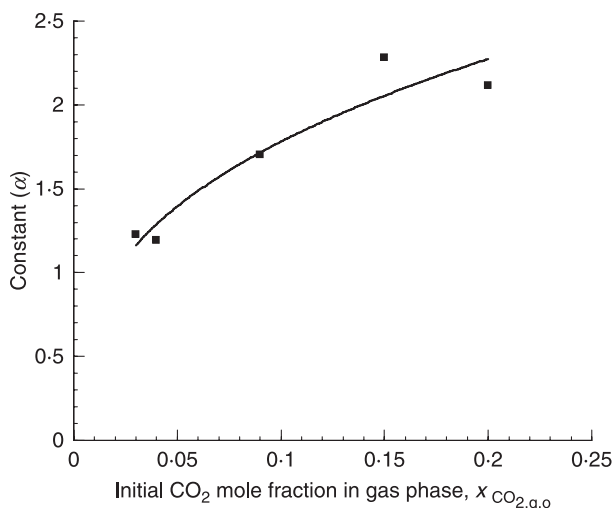


Figure 7 (a) The constant α in eqn (10) as a function of $x_{\text{CO}_2,\text{g},0}$. The solid line corresponds to $\alpha = 4x_{\text{CO}_2,\text{g},0}^{0.35}$.

Hydrogen and oxygen productions

Figure 9a shows the concentration of hydrogen measured in the head-space as a function of the dimensionless time $t/t_{1/2}$ for all runs. It indicates that the maximum hydrogen concentration is achieved at high irradiance. Moreover, the concentration of hydrogen accumulated in the head-space normalized with its maximum value $C_{\text{H}_2,\text{g,max}}$ as a function of dimensionless time $t/t_{1/2}$ for irradiance larger than 7000 lux is shown in Fig. 9b. It establishes that $C_{\text{H}_2,\text{g}}/C_{\text{H}_2,\text{g,max}}$ varies exponentially with $t/t_{1/2}$ and can be expressed as:

$$\frac{C_{\text{H}_2,\text{g}}(t)}{C_{\text{H}_2,\text{g,max}}} = \exp \left[4.45 \left(\frac{t}{t_{1/2}} \right) - 6.1 \right] \quad (14)$$

Similarly, Fig. 10a, b show the oxygen concentration and the normalized oxygen concentration with its maximum value, respectively, as functions of the dimensionless time $t/t_{1/2}$ for all runs. Figure 10(b) indicates that the normalized oxygen concentration varies exponentially with $t/t_{1/2}$ according to:

$$\frac{C_{\text{O}_2,\text{g}}(t)}{C_{\text{O}_2,\text{g,max}}} = \exp \left[2.25 \left(\frac{t}{t_{1/2}} \right) - 3.5 \right] \quad (15)$$

To use eqns (14) and (15) to determine the evolution of oxygen and hydrogen concentrations, the maximum concentrations $C_{\text{O}_2,\text{g,max}}$ and $C_{\text{H}_2,\text{g,max}}$ must be expressed in terms of the initial CO₂ mole fraction $x_{\text{CO}_2,\text{g},0}$ and irradiance G . Figure 11 shows that $C_{\text{O}_2,\text{g,max}}$ is independent of irradiance and varies linearly with $x_{\text{CO}_2,\text{g},0}$ according to:

$$C_{\text{O}_2,\text{g,max}} = 3.45x_{\text{CO}_2,\text{g},0} \quad (16)$$

with a correlation coefficient $R^2=0.94$. This demonstrates that the oxygen yield of *A. variabilis*, i.e. the mass of O₂ produced per mass of CO₂ consumed, was constant for the parameters explored.

Figure 12a shows $C_{\text{H}_2,\text{g,max}}$ as a function of both irradiance and of the initial CO₂ mole fraction. It indicates that within the parameter ranges explored, the optimum irradiance for maximum H₂ production was around 10 000 lux. Figure 12b shows $C_{\text{H}_2,\text{g,max}}$ as a function of $x_{\text{CO}_2,\text{g},0}$ for irradiances larger than 7000 lux for which H₂ production is the largest. It indicates that $C_{\text{H}_2,\text{g,max}}$ increases with increasing $x_{\text{CO}_2,\text{g},0}$. As a first order approximation, the relationship between $C_{\text{H}_2,\text{g,max}}$ and $x_{\text{CO}_2,\text{g},0}$ can be written as:

$$C_{\text{H}_2,\text{g,max}} = 1.50 \times 10^{-2}x_{\text{CO}_2,\text{g},0} - 3.75 \times 10^{-4} \quad (17)$$

for $G \geq 7000$ lux

with a correlation coefficient R^2 of 0.75.

Discussion

Kinetic models describing the cyanobacterial growth, carbon uptake, and O₂ production depend on the specific growth rate μ which is a function of the instantaneous available irradiance G_{av} and total dissolved inorganic carbon concentration C_{TOT} . In an earlier study, Badger and Andrews (1982) suggested that both H₂CO₃^{*} and HCO₃⁻ can act as substrate for cyanobacteria. Furthermore, Goldman *et al.* (1974) used C_{TOT} given by eqn (5) in the Monod model to successfully predict algal growth in carbon limited conditions for pH between 7.05 and 7.61. More recently, Erickson *et al.* (1987) modelled the growth rate of the cyanobacteria *S. platensis* under light and inorganic carbon limited conditions using the Monod model. Table 3 indicates that the parameters they reported for *S. platensis* agree well with those obtained in the present study for *A. variabilis*. Note that Erickson *et al.* (1987) expressed the Monod model only in terms of HCO₃⁻ concentration as opposed to C_{TOT} . However, it is equivalent to using C_{TOT} as the pH was kept constant and equal to 9.2. Then, the ratio of HCO₃⁻ to H₂CO₃^{*} concentrations is about 800 while CO₃²⁻ concentration is negligibly small. In other words, at pH 9.2, C_{TOT} is approximately equal to the HCO₃⁻ concentration. In the present study, the pH varies from 6.6 to 7.4 and the ratio of HCO₃⁻ to H₂CO₃^{*} concentration varies between 2 and 12. Therefore, both species need to be accounted for in computing C_{TOT} to be used in eqn (2). Furthermore, the aforementioned studies did not account for the inhibitory effect of dissolved inorganic carbon (i.e. $K_I = \infty$) as the

concentration of inorganic carbon was low, $C_{TOT} < 0.67 \times 10^{-3} \text{ kmol C m}^{-3}$. However, in the present study, the inorganic carbon concentration reached up to $C_{TOT} < 20 \times 10^{-3} \text{ kmol C m}^{-3}$ and ignoring the carbon inhibition effects in eqn (2) resulted in poor model predictions. The values of the retrieved parameters μ_{max} , K_G , and K_C agree with those reported by Erickson *et al.* (1987) and are valid for low carbon concentrations. In addition, the inhibitory effect of large inorganic carbon concentration is successfully accounted for by the modified Monod model through the parameter K_I .

Moreover, due to the fact that CO₂ consumption and O₂ production are mainly growth related processes, their evolution has been successfully modelled using the specific growth rates. On the other hand, H₂ evolution is a much more complex process. It depends on the active enzyme concentration, the O₂ concentration in the medium, the irradiance, as well as the growth rate. Therefore, simple models similar to eqns (6) or (7) could not model all data within $\pm 30\%$.

Furthermore, these models assume that the irradiance within the culture and the concentration of the dissolved inorganic carbon are known while they cannot be measured directly. Consequently, in the second part of this paper a new analysis for CO₂ consumption, cyanobacterial growth, as well as hydrogen and oxygen productions as functions of $t_{1/2}$ has been developed. Experimental data indicates that $t_{1/2}$ is a relevant time scale for CO₂ consumption, growth, H₂ and O₂ production. The simplicity of this analysis resides in the fact that it depends on directly measurable and controllable quantities. Furthermore, it can be used to determine the light saturation of photosynthesis as shown in Fig. 4. However, the applicability of this scaling analysis is limited to systems having (i) the same initial cyanobacteria concentration and (ii) similar pH.

Moreover, Fig. 8a establishes that an optimum $x_{CO_{2,g,o}}$ around 0.05 exists for maximum average specific growth rate for all irradiances. Moreover, it shows that the average specific growth rate increases with increasing irradiance. Yoon *et al.* (2002) reported that for experiments conducted at 30°C with $x_{CO_{2,g,o}}$ around 0.11 the average specific growth rate decreased from 0.054 to 0.046 h⁻¹ for *A. variabilis* as the irradiance increased from 3500 to 7000 lux. In the present study at 24°C with initial CO₂ mole fraction of 0.11, μ_{avg} increased from 0.028 to 0.038 h⁻¹ for the same increase in irradiance. The observed discrepancy between the results reported in this study and those reported by Yoon *et al.* (2002) can be attributed to the combination of the differences in pH and in temperature.

Furthermore, Fig. 8b shows that the average specific CO₂ uptake rate exhibits similar trends to those of the

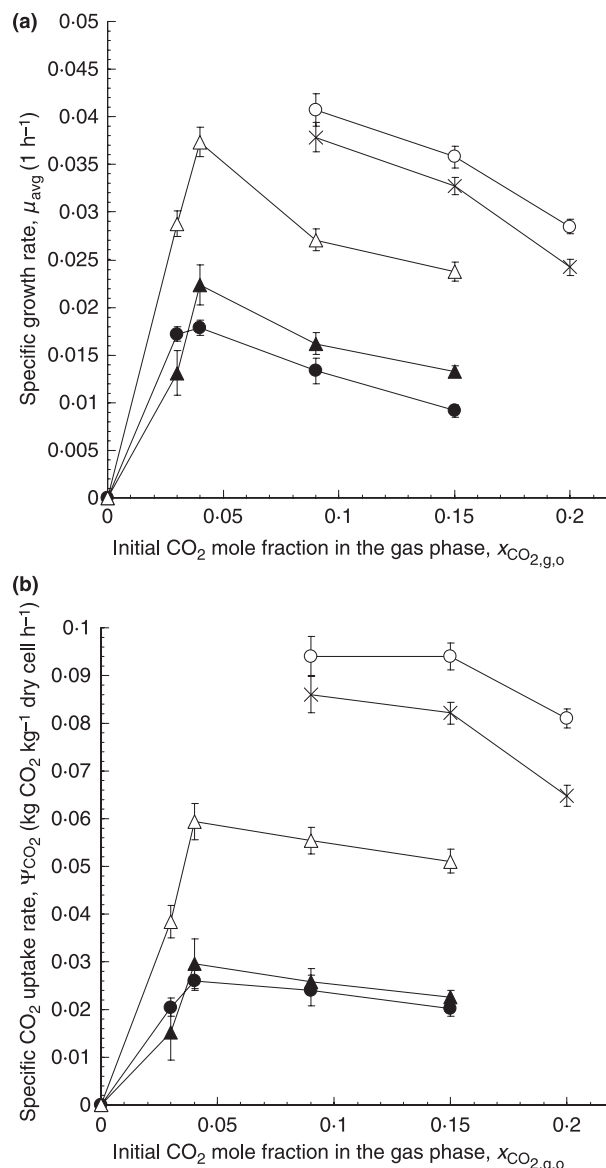


Figure 8 (a) The average specific growth rate μ_{avg} , and (b) the average specific CO₂ uptake rate ψ_{CO_2} of *Anabaena variabilis* as functions of $x_{CO_{2,g,o}}$ at all irradiances: (●) 1100–1200 lux, (▲) 1700–1800 lux, (△) 4000–5000 lux, (×) 7000–8000 lux and (○) 15 000–16 000 lux.

average specific growth rate with an optimum $x_{CO_{2,g,o}}$ around 0.05 for maximum ψ_{CO_2} . Yoon *et al.* (2002) reported an average specific CO₂ uptake rate ψ_{CO_2} of about 0.130 kg CO₂ kg⁻¹ dry cell h⁻¹ for $x_{CO_{2,g,o}}$ around 0.05 and irradiance around 4000 lux, whereas, in the present study, it was only 0.060 kg CO₂ kg⁻¹ dry cell h⁻¹ under the same irradiance and $x_{CO_{2,g,o}}$. The difference can be attributed to the fact that the experiments of the present study were conducted at 24°C instead of 30°C (Yoon *et al.* 2002). It is apparent that

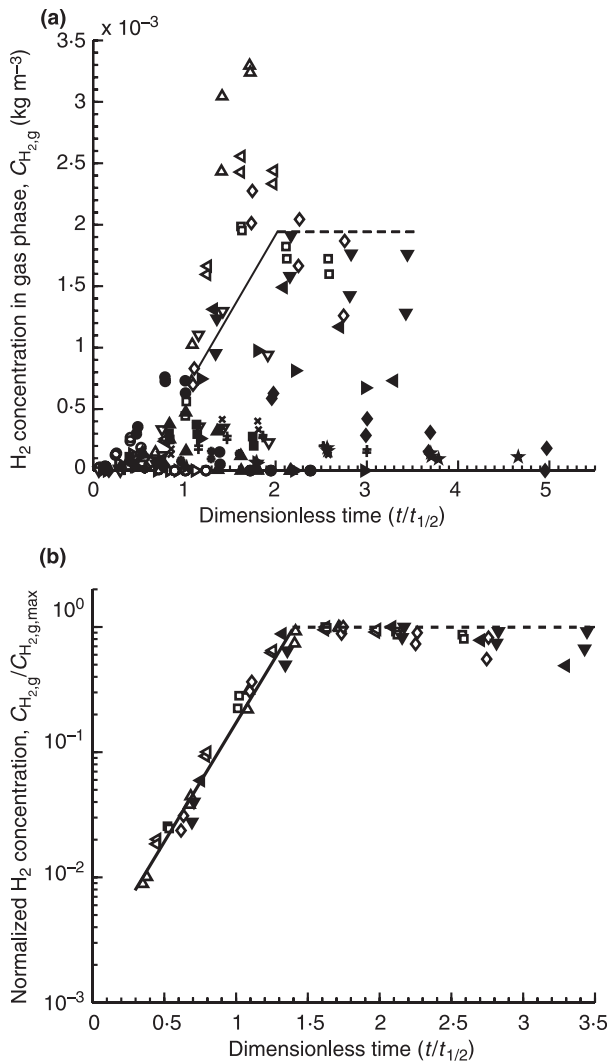


Figure 9 Concentration of hydrogen accumulated in the head-space (a) for all tests vs dimensionless time $t/t_{1/2}$, (b) normalized with the maximum concentration produced vs dimensionless time $t/t_{1/2}$ for irradiance $G \geq 7000$ lux. The solid line corresponds to $C_{H_2,g}/C_{H_2,g,max} = \exp[4.45(t/t_{1/2}) - 6.1]$. (Δ) 0GH, (\triangleleft) 0IJ, (\triangleright) 1AB, (\circ) 1CD, (∇) 1EF, (\square) 1GH, (\diamond) 1IJ, (\blacktriangle) 2AB, (\bullet) 2CD, (\blacktriangleleft) 2EF, (\blacktriangleright) 2GH, (\blacktriangleright) 2IJ, (\blacksquare) 3AB, (\times) 3CD, (\blacklozenge) 3EF, ($+$) 4AB, (\star) 4CD, (\star) 4EF.

increasing the temperature enhances the CO₂ uptake metabolism of *A. variabilis* as confirmed by Tsygankov *et al.* (1999). Note that due to experimental difficulties in capturing fast CO₂ consumption rate with the available equipment and procedure, no experiments were conducted for initial CO₂ mole fraction less than 0.08 at irradiances higher than 5000 lux.

Figures 9 and 10 show that H₂ and O₂ concentrations in the headspace increases exponentially during the growth phase. Due to the presence of nitrate in the medium (initially about 20 mmol l⁻¹), the nitrogenase activity is expected to be low (Madamwar *et al.* 2000). Moreover,

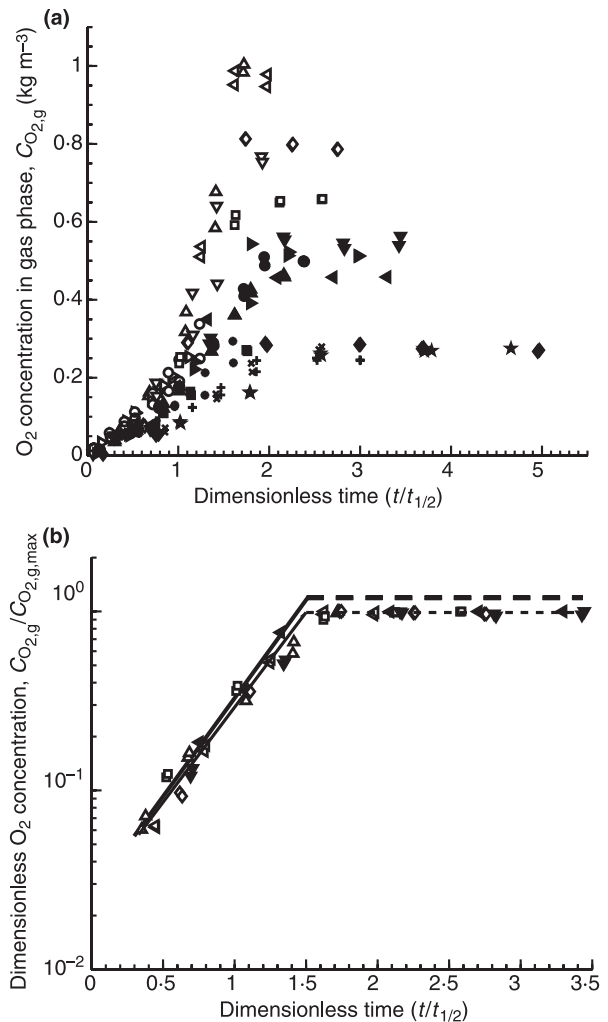


Figure 10 Concentration of oxygen accumulated in the head-space for (a) all tests vs dimensionless time $t/t_{1/2}$, (b) normalized with the maximum concentration produced vs dimensionless time $t/t_{1/2}$ for irradiance $G \geq 7000$ lux. The solid line corresponds to $C_{O_2,g}/C_{O_2,g,max} = \exp[2.25(t/t_{1/2}) - 3.5]$. (Δ) 0GH, (\triangleleft) 0IJ, (\triangleright) 1AB, (\circ) 1CD, (∇) 1EF, (\square) 1GH, (\diamond) 1IJ, (\blacktriangle) 2AB, (\bullet) 2CD, (\blacktriangleleft) 2EF, (\blacktriangleright) 2GH, (\blacktriangleright) 2IJ, (\blacksquare) 3AB, (\times) 3CD, (\blacklozenge) 3EF, ($+$) 4AB, (\star) 4CD, (\star) 4EF.

H₂ production using the nitrogenase enzyme is not expected to stop when the growth stops or slows down such as during two stage H₂ production (Yoon *et al.* 2002). However, increased concentration of evolved O₂ could have inhibited H₂ production. In addition, the initial anaerobic conditions promotes the bidirectional hydrogenase activity. Therefore, the observed H₂ production during the experiments is expected to be due to the bidirectional hydrogenase activity. Furthermore, the decrease in the H₂ concentration for $t/t_{1/2} > 1.5$ can be attributed to consumption of the produced H₂ due to the presence of uptake hydrogenase (Tsygankov *et al.* 1998).

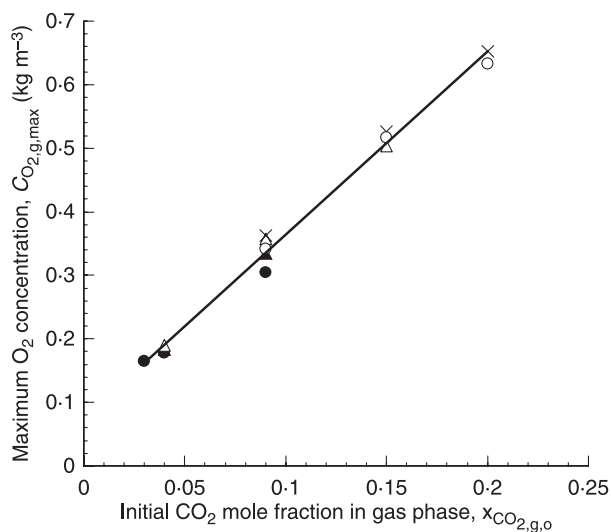


Figure 11 Maximum concentration of oxygen accumulated in the head-space $C_{O_2,g,max}$ as a function of the $x_{CO_2,g,o}$ for (●) 1100–1200 lux, (▲) 1700–1800 lux, (△) 4000–5000 lux, (×) 7000–8000 lux and (○) 15 000–16 000 lux. The solid line corresponds to $C_{O_2,g,max} = 3.45x_{CO_2,g,o}$.

However, unlike hydrogen, the oxygen concentration does not decrease appreciably beyond the exponential growth phase. Finally, $C_{H_2,g}$ and $C_{O_2,g}$ reach their maximum at dimensionless time $t/t_{1/2}$ equal to 1.37 and 1.55, respectively, and shortly before the CO₂ concentration vanishes at $t/t_{1/2}$ equal to 1.8. Note that the reported values of CO₂, O₂, and H₂ values correspond to the net produced or consumed quantities as it is difficult to experimentally distinguish the contribution of each phenomenon. In particular, CO₂ is being consumed during photosynthesis and being produced during respiration and possibly during H₂ production, provided H₂ production is catalyzed by nitrogenase (Das and Veziroglu 2001). Similarly, O₂ is being produced during photosynthesis and consumed during respiration.

Figures 11 and 12 show the maximum O₂ and H₂ concentrations attained in the headspace as functions of $x_{CO_2,g,o}$ for different irradiances. Unlike for $C_{O_2,g,max}$, it is difficult to establish a simple and reliable relationship between $C_{H_2,g,max}$ and the parameters G and $x_{CO_2,g,o}$ due to the complexity of the hydrogen metabolism of *A. variabilis*. This complexity arises because (i) the hydrogen production is a strong function of both the irradiance G and the initial CO₂ concentration (Markov *et al.* 1997a) and (ii) the produced hydrogen is being consumed back by the micro-organisms at a rate comparable to the production rate of hydrogen (Tsygankov *et al.* 1998). Tsygankov *et al.* (1998) reported that the wild strain *A. variabilis* ATCC 29413 did not produce any hydrogen in the

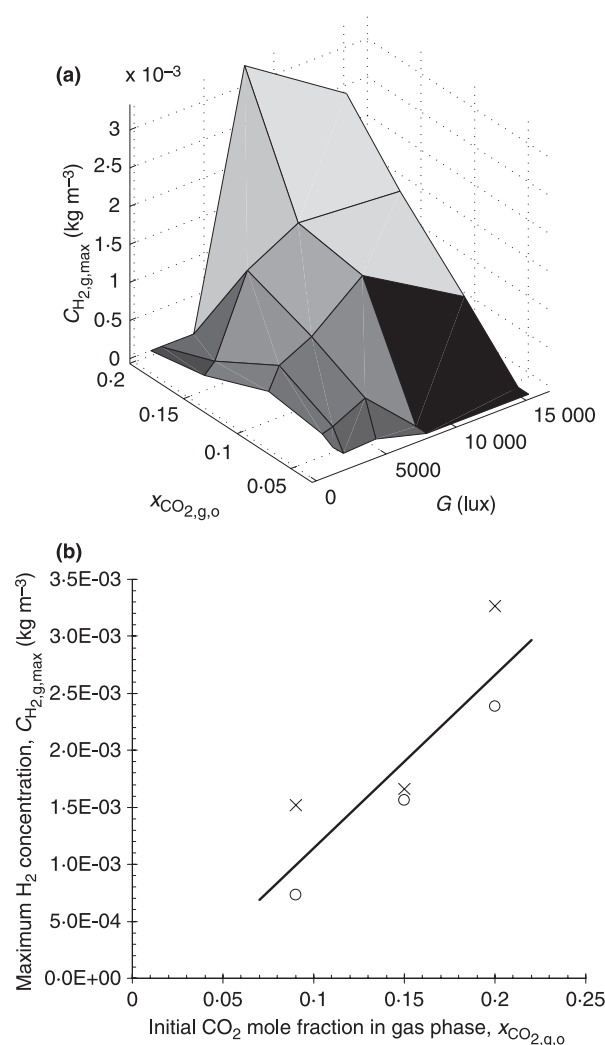


Figure 12 (a) Maximum concentration of hydrogen accumulated in the head-space as a function of the initial CO₂ mole fraction and irradiance. (b) $C_{H_2,g,max}$ as a function of $x_{CO_2,g,o}$ for two of the highest irradiances for (×) 7,000–8,000 lux and (○) 15 000–16 000 lux. The solid line corresponds to $C_{H_2,g,max} = 1.50 \times 10^{-2}x_{CO_2,g,o} - 3.75 \times 10^{-4}$.

presence of CO₂ in the atmosphere. In contrast, the present study indicates that hydrogen production by the wild strain is possible under argon and CO₂ atmosphere albeit at a lower production rate. Indeed, the maximum hydrogen production observed in our experiments was 0.3 mmol kg⁻¹ dry cell h⁻¹ whereas reported rates for wild *A. variabilis* strains range from 5.58 mmol kg⁻¹ dry cell h⁻¹ in dark fermentation (Shah *et al.* 2001), 165 mmol kg⁻¹ dry cell h⁻¹ in a multi stage photobioreactor (Yoon *et al.* 2006), and to 720 mmol kg⁻¹ dry cell h⁻¹ under nutritional stress (Sveshnikov *et al.* 1997). The low hydrogen production rates observed in the present study are attributed to (i) CO₂ fixation and H₂

production processes competing for the reductants generated from water splitting (Prince and Kheshgi 2005); (ii) the presence of nitrate in the medium (Shah *et al.* 2001); and (iii) the consumption of the produced H₂ by the wild strain *A. variabilis* at high dissolved O₂ concentrations (Tsygankov *et al.* 1998).

Conclusions

A parametric experimental study has been performed to assess the CO₂ consumption, growth, H₂ and O₂ productions of the cyanobacteria *A. variabilis* ATCC 29413-UTM in batch experiment. The main parameters are the irradiance and the initial CO₂ mole fraction in the head-space. The micro-organisms were grown in atmosphere containing argon and CO₂, at a pH of 7.0 ± 0.4 with nitrate in the medium. A new scaling analysis for CO₂ consumption, growth, and H₂ and O₂ production is presented. Under the conditions presented in this study, the following conclusions can be drawn for *A. variabilis*,

1. Kinetic equations based on the Monod model are used to model the growth, carbon uptake, and O₂ production by *A. variabilis* taking into account (i) light saturation; (ii) CO₂ saturation; and (iii) CO₂ inhibition. The parameters obtained agree well with values reported for other cyanobacteria (Erickson *et al.* 1987) at low inorganic carbon concentrations and expands the model to large concentrations when growth inhibition occurs. The experimental data falls within 30% of the model predictions. However, similar approach could not predict experimental data for H₂ production rate.
2. The CO₂ consumption half-time, defined as the time when the CO₂ mole fraction in the gas phase decreases to half of its initial value, is a relevant time scale for CO₂ consumption, growth, H₂ and O₂ production. It depends on the total irradiance incident on the vials and the initial CO₂ mole fraction.
3. The scaling analysis facilitates the determination of the saturation irradiance which is found to be 5170 lux.
4. For maximum specific CO₂ consumption and specific growth rates, the optimum initial CO₂ mole fraction in the gas phase is about 0.05 for any irradiance between 1000 and 16 000 lux.
5. Optimum irradiance for maximum H₂ production has been found to be around 10 000 lux despite the low overall H₂ production rates.
6. Neither the CO₂ consumption nor the growth rate was inhibited by irradiance up to about 16 000 lux.

Finally, the kinetic equations can be used in simulations for optimizing the operating conditions of a photobioreactor for rapid growth and maximum CO₂ mitigation. Moreover, it is expected that the above experimental and scaling analysis method can be used for

analyzing other CO₂ mitigating and H₂ producing micro-organisms.

Acknowledgements

The authors gratefully acknowledge the support of the California Energy Commission through the Energy Innovation Small Grant (EISG 53723A/03-29; Project Manager: Michelle McGraw). They are indebted to Chu Ching Lin, Edward Ruth, Jong Hyun Yoon, and Dr James C. Liao for their helpful discussions and exchanges of information.

Nomenclature

C	volumetric mass concentration, kg m ⁻³ ;
C_{TOT}	molar concentration of total dissolved inorganic carbon, kmol m ⁻³ ;
$E_{\text{ext},\lambda}$	spectral extinction cross-section, m ² kg ⁻¹ dry cell;
$E_{\text{ext,PAR}}$	average extinction cross-section over the PAR, m ² kg ⁻¹ dry cell;
G	local irradiance, lux;
G_{av}	average irradiance within the culture in the spectral range from 400 to 700 nm, lux;
G_{in}	total incident irradiance in the spectral range from 400 to 700 nm, lux;
K_C	half-saturation constant for dissolved inorganic carbon, kmol m ⁻³ ;
K_G	half-saturation constant for light, lux;
K_I	inhibition constant for dissolved inorganic carbon, kmol m ⁻³ ;
L	depth of the cyanobacteria suspension in the vial, m;
OD	optical density;
t	time, h;
$t_{1/2}$	half-time, h;
X	cyanobacteria concentration, kg dry cell m ⁻³ ;
$X_{\text{avg},\Delta t}$	average cyanobacteria concentration in the time interval Δt , kg dry cell m ⁻³ ;
x	mole fraction;
$Y_{X/C}$	biomass yield based on carbon, kg dry cell kmol ⁻¹ C;
Y_{X/CO_2}	biomass yield based on CO ₂ , kg dry cell kg ⁻¹ CO ₂ ;
$Y_{\text{O}_2/X}$	O ₂ yield based on biomass, kg O ₂ kg ⁻¹ dry cell;
z	location in the cyanobacteria suspension measured from the liquid surface, m.

Greek symbols

α	exponential constant;
β	slope of half-time vs initial CO ₂ mole fraction in the gas phase, h;
$\mu_{\Delta t}$	specific growth rate in the time interval Δt , h ⁻¹ ;
μ_{avg}	average specific growth rate, h ⁻¹ ;
μ_{max}	maximum specific growth rate, h ⁻¹ ;
ψ_{CO_2}	average specific CO ₂ uptake rate, kg CO ₂ kg ⁻¹ dry cell h ⁻¹ .

Subscripts

CO ₂	refers to carbon dioxide;
<i>g</i>	refers to gas phase;
H ₂	refers to hydrogen;
<i>i</i>	refers to a gas species;
<i>L</i>	refers to liquid phase;
max	refers to the maximum amount of a gas species produced by the cyanobacteria;
O ₂	refers to oxygen;
o	refers to initial conditions.

References

- Asenjo, J. and Merchuk, J. (1995) *Bioreactor System Design*. New York, NY: Marcel Dekker.
- Badger, M. and Andrews, T. (1982) Photosynthesis and inorganic carbon usage by the marine cyanobacterium *Synechococcus* sp. *Plant Physiol* **70**, 517–523.
- Benemann, J. (2000) Hydrogen production by microalgae. *J Appl Phycol* **12**, 291–300.
- Benjamin, M. (2002) *Water Chemistry*. New York, NY: McGraw Hill.
- Berberoğlu, H. and Pilon, L. (2007). Experimental measurement of the radiation characteristics of *Anabaena variabilis* ATCC 29413-U and *Rhodospira rubra* ATCC 49419. *Int J Hydrogen Energy*, in press.
- Berberoğlu, H., Yin, J. and Pilon, L. (2007) Simulating light transfer in a bubble sparged photobioreactor for simultaneous hydrogen fuel production and CO₂ mitigation. *Int J Hydrogen Energy* **32**, 2273–2285.
- Borodin, V., Tsygankov, A., Rao, K. and Hall, D. (2000) Hydrogen Production by *Anabaena variabilis* PK84 under simulated outdoor conditions. *Biotechnol Bioeng* **69**, 478–485.
- Das, D. and Veziroglu, T. (2001) Hydrogen Production by biological processes: a survey of literature. *Int J Hydrogen Energy* **26**, 13–28.
- Dunn, I., Heinzle, E., Ingham, J. and Prenosil, J. (2003) *Biological Reaction Engineering; Dynamic Modelling Fundamentals with Simulation Examples*, 2nd edn. Germany: Wiley-VCH.
- Erickson, L., Curless, C. and Lee, H. (1987) Modeling and simulation of photosynthetic microbial growth. *Ann NY Acad Sci* **506**, 308–324.
- Goldman, J., Oswald, W. and Jenkins, D. (1974) The kinetics of inorganic carbon limited algal growth. *J Water Pollut Control Fed* **46**, 554–574.
- Hansel, A. and Lindblad, P. (1998) Towards optimization of cyanobacteria as biotechnologically relevant producers of molecular hydrogen, a clean and renewable energy source. *Appl Microbiol Biotechnol* **50**, 153–160.
- Happe, T., Schutz, K. and Bohme, H. (2000) Transcriptional and mutational analysis of the uptakehydrogenase of the filamentous cyanobacterium *Anabaena variabilis* ATCC 29413. *J Biotechnol* **182**, 1624–1631.
- Joint Genome Institute (2007) US Department of Energy, Office of Science. Available at: <http://www.jgi.doe.gov> (accessed on: April 19, 2007).
- Madamwar, D., Garg, N. and Shah, V. (2000) Cyanobacterial hydrogen production World. *J Microbiol Biotechnol* **16**, 757–767.
- Markav, S., Lichtl, R., Rao, K. and Hall, D. (1993) A hollow fibre photobioreactor for continuous production of hydrogen by immobilized cyanobacteria under partial vacuum. *Int J Hydrogen Energy* **18**, 901–906.
- Markov, S., Bazin, M. and Hall, D. (1995) Hydrogen photoproduction and carbon dioxide uptake by immobilized *Anabaena variabilis* in a hollow-fiber photobioreactor. *Enzyme Microb Technol* **17**, 306–310.
- Markov, S., Thomas, A., Bazin, M. and Hall, D. (1997a) Photoproduction of hydrogen by cyanobacteria under partial vacuum in batch culture or in a photobioreactor. *Int J Hydrogen Energy* **22**, 521–524.
- Markov, S., Weaver, P. and Seibert, M. (1997b) Spiral tubular bioreactors for hydrogen production by photosynthetic microorganisms—design and operation. *Appl Biochem Biotechnol* **63–65**, 577–584.
- Merzlyak, M. and Naqvi, K. (2000) On recording the true absorption spectrum and scattering spectrum of a turbid sample: application to cell suspensions of cyanobacterium *Anabaena variabilis*. *J Photochem Photobiol B* **58**, 123–129.
- Pinto, F., Troshina, O. and Lindblad, P. (2002) A brief look at three decades of research on cyanobacterial hydrogen evolution. *Int J Hydrogen Energy* **27**, 1209–1215.
- Prince, R.C. and Kleshgi, H.S. (2005) The photobiological production of hydrogen: potential efficiency and effectiveness as a renewable fuel. *Crit Rev Microbiol* **31**, 19–31.
- Shah, V., Garg, N. and Madamwar, D. (2001) Ultrastructure of the fresh water cyanobacterium *Anabaena variabilis* SPU 003 and its application for oxygen-free hydrogen production. *FEMS Microbiol Lett* **194**, 71–75.
- Smith, L., McCarthy, P. and Kitanidis, P. (1998) Spreadsheet method for evaluation of biochemical reaction rate coefficients and their uncertainties by weighted nonlinear least-squares analysis of the integrated monod equation. *Appl Environ Microbiol* **64**, 2044–2050.

- Sveshnikov, D., Sveshnikova, N., Rao, K. and Hall, D. (1997) Hydrogen metabolism of mutant forms of *Anabaena variabilis* in continuous cultures and under nutritional stress. *FEMS Microbiol Lett* **147**, 297–301.
- Tsygankov, A., Serebryakova, L., Rao, K. and Hall, D. (1998) Acetylene reduction and hydrogen photoproduction by wild-type and mutant strains of *Anabaena* at different CO₂ and O₂ concentrations. *FEMS Microbiol Lett* **167**, 13–17.
- Tsygankov, A., Bordin, V., Rao, K. and Hall, D. (1999) H₂ photoproduction by batch culture of *Anabaena variabilis* ATCC 29413 and its mutant PK84 in a photobioreactor. *Biotechnol Bioeng* **64**, 709–715.
- Tsygankov, A., Fedorov, A., Kosourov, S. and Rao, K. (2002) Hydrogen production by cyanobacteria in an automated outdoor photobioreactor under aerobic conditions. *Biotechnol Bioeng* **80**, 777–783.
- Yoon, J., Sim, S., Kim, M. and Park, T. (2002) High cell density culture of *Anabaena variabilis* using repeated injections of carbon dioxide for the production of hydrogen. *Int J Hydrogen Energy* **27**, 1265–1270.
- Yoon, J., Shin, J., Kim, M., Sim, S. and Park, T. (2006) Evaluation of conversion efficiency of light to hydrogen energy by *Anabaena variabilis*. *Int J Hydrogen Energy* **31**, 721–727.